

Screening of magnetic moments in PuAm alloy : LDA+DMFT study

J. H. Shim¹, K. Haule¹, S. Savrasov², and G. Kotliar¹

¹ *Department of Physics, Rutgers University, Piscataway, NJ 08854, USA and*

² *Department of Physics, University of California, Davis, CA 95616*

(Dated: September 15, 2021)

The puzzling absence of Pu magnetic moments in a PuAm environment is explored using the self-consistent Dynamical Mean Field Theory (DMFT) calculations in combination with the Local Density Approximation. We argue that δ -Pu-Am alloys provide an ideal test bed for investigating the screening of moments from the single impurity limit to the dense limit. Several important effects can be studied: volume expansion, shift of the bare Pu on-site f energy level, and the reduction of the hybridization cloud resulting from the collective character of the Kondo effect in the Anderson lattice. These effects compensate each other and result in a coherence scale, which is independent of alloy composition, and is around 800 K. We emphasize the role of the DMFT self-consistency condition, and multiplet splittings in Pu and Am atoms, in order to capture the correct value of the coherence scale in the alloy.

PACS numbers:

The electronic structure of plutonium (Pu) is one of the outstanding issues in condensed matter theory. The volume of δ -Pu is between that of the early actinides, where the f electrons are itinerant, and the late actinides, where the f electrons are localized. Hence the view that the f electrons are very close to a localization-delocalization transition was put forward early on by Johansson¹.

Theoretical density functional theory calculations in many implementations, all predict δ -Pu to be magnetic². Nevertheless, various experiments that searched for the magnetic moment in δ -Pu, such as specific heat in field, neutron scattering and μ SR measurements^{3,4}, found no evidence for the ordered, or fluctuating moment in the energy and temperature windows probed by these experiments. High energy spectroscopies, such as electron-energy-loss spectroscopy and X-ray absorption spectroscopy experiments of the $5d$ - $5f$ core-valence transition, clearly indicate that f electrons in Pu are in a $5f^5$ configuration⁵, which carries a magnetic moment. Reconciling these low energy and high energy experiments, has led to numerous conflicting theories. Within the most recent Dynamical Mean Field Theory (DMFT) studies of δ -Pu, allowing for magnetic and non magnetic solutions, Pu does not order magnetically, and instead forms a non-magnetic Fermi liquid with a coherence temperature T^* of the order of 800 K⁶. The Pu atoms are in a mixed valent state, with a dominant $5f^5$ configuration, but with sizeable admixture of $5f^6$. On the basis of this picture it was expected, and shown explicitly via a landmark continuous-time quantum Monte Carlo calculation⁷, that expanding the lattice would reduce the coherence temperature T^* , making the moment of the f^5 configuration observable. Other theories, whereby the f moments are quenched directly by spin pairing, which is mediated by the spin orbit coupling, also account for the absence of moments in Pu, and suggest that this material is at a quantum critical point⁸.

PuAm alloy is a unique system to study the effect of lattice expansion of δ -Pu since the volume of Americium

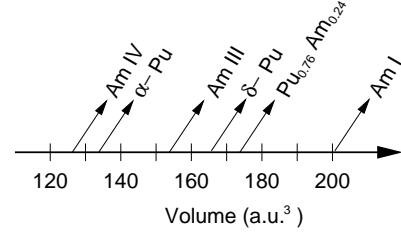


FIG. 1: The volume of Pu and Am in each phases. According to Ref. 9, the volume of $\text{Pu}_{0.76}\text{Am}_{0.24}$ is located slightly above ($\sim 2\%$) the value estimated from the linear interpolation between δ -Pu and Am-I.

at ambient pressure (Am-I) is 20% bigger than volume of δ -Pu (see Fig. 1). Moreover, there is no structural phase transition between pure δ -Pu and $\text{Pu}_{0.25}\text{Am}_{0.75}$, and the structure remains fcc ¹⁰. Surprisingly, an intensive program studying the Pu-Am mixtures, which has the effect of expanding the distance between the Pu atoms, has not shown an enhanced magnetic susceptibility, nor a narrowing of the peak at the Fermi level, as measured by photoemission experiment^{9,11}. This seems naively at odds with both the quantum critical picture, and the DMFT picture, and supports the suggestion, that the configuration of Pu in the solid is close to an inert $5f^6$ configuration^{12,13}, being essentially equivalent to Am configuration. Unfortunately, this picture can not explain the results of high energy spectroscopies⁵, nor the difference in specific heat between α -Pu and δ -Pu^{6,14}, nor the spectral properties¹⁵. Hence the puzzle of the absence of magnetic moments in Pu-Am alloys remains.

In this paper, we provide a theoretical explanation of this puzzle using LDA+DMFT method^{16,17}. We find that indeed the moment remains well screened in agreement with experiment, and we identify the mechanism that compensates the effects of the lattice expansion. While the Pu-Am system cannot realize the unscreening of the local moment, and hence the approach to quantum

criticality, it provides an ideal system in which to follow the transition from collective screening of moments, to single impurity spin screening of moments.

Within the LDA+DMFT method¹⁷, the itinerant *spd* electrons are treated by the LDA method¹⁸, while for the electrons in the correlated *f* orbitals, all the local Feynman diagrams are summed up by solving an auxiliary quantum impurity problem, subject to a DMFT self-consistency condition

$$\frac{1}{\omega + \mu - E_{imp} - \Sigma - \Delta} = \sum_{\mathbf{k}} [G_{\mathbf{k}}(\omega)]_{ff}. \quad (1)$$

Here $\Delta(\omega)$ is the hybridization matrix of the auxiliary impurity problem, E_{imp} is the matrix of impurity levels, and $G_{\mathbf{k}}$ is the one electron Green's function $G_{\mathbf{k}} = 1/(O_{\mathbf{k}}(\omega + \mu) - H_{\mathbf{k}} - \Sigma)$. $H_{\mathbf{k}}$ and $O_{\mathbf{k}}$ are the LDA Hamiltonian and the overlap matrix in the projective orthogonalized LMTO basis set¹⁹. The quantum impurity solver is used to determine the local self-energy correction to the *f*-orbital Hamiltonian, which is a functional of the impurity levels, and the hybridization strength $\Sigma[E_{imp}, \Delta]$. To solve the impurity problem, we used the vertex corrected one-crossing approximation method²⁰, and the results are further cross-checked by the continuous time quantum Monte Carlo method²¹. The Slater integrals F^k ($k = 2, 4, 6$) are computed by Cowan's atomic Hartree-Fock program including relativistic corrections²² and rescaled to 80% of their atomic value, accounting for the screening in the solid. We use Coulomb interaction $U = 4.5$ eV, consistent with previous studies of Pu and Am^{23,24}.

The $\text{Pu}_{1-x}\text{Am}_x$ alloys are approximated by the charge ordered compounds with $x = 0, 1/4, 1/2$, and $3/4$. Based on the original *fcc* phase, we use a four times larger unit cell with the simple cubic structure. To determine the lattice constant of the alloy, we used the linear interpolation between the two end compounds, δ -Pu and β -Am⁹. We use $8 \times 8 \times 8$ momentum points in the first Brillouin zone in combination with the tetrahedron method.

Figure 2 (a-e) shows the calculated spectral function of $\text{Pu}_{1-x}\text{Am}_x$. The theoretical results are compared to the experimental spectra of δ -Pu alloyed with Am⁹. Naively, one would expect that alloys of Pu and Am are magnetic, because the volume of the alloy is bigger than the volume of the elemental plutonium. Increasing the volume decreases the hybridization between the *5f*-orbital and the conduction *spd*-orbitals, and consequentially the Kondo coupling J should be reduced. Since the strength of the Kondo screening depends exponentially on the Kondo coupling J while RKKY scale is only a quadratic function of J , one is expecting the screening to become inefficient even for a small change of J . However, experiments ruled out the possibility of magnetic moment formation. The specific heat of $\text{Pu}_{1-x}\text{Am}_x$ does not show any significant changes¹¹ with alloying and is simply proportional to the Pu content. This is because the inert f^6 configuration of Am has very small specific heat, and only Pu atoms contribute to c_v . The photoemission spectral of $\text{Pu}_{1-x}\text{Am}_x$

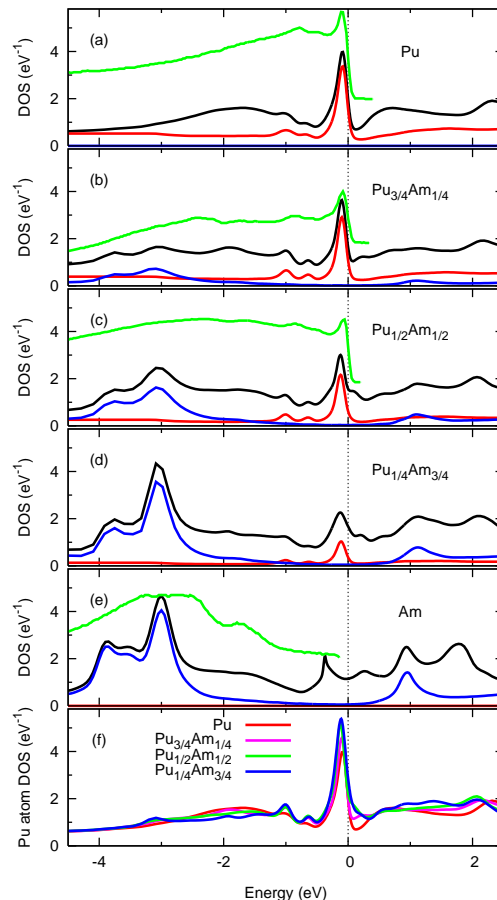


FIG. 2: (a-e) The spectral function of $\text{Pu}_{1-x}\text{Am}_x$ in the *fcc* unit cell. Total (black), Pu 5*f* (red), Am 5*f* (blue) spectrum are obtained by the LDA+DMFT method. The green lines show experimental photoemission spectrum at $x = 0.0$ (a), 0.20 (b), 0.36 (c), and 1.0 (e) (extracted from Ref. 9). (f) The spectral function of Pu atom for various Am dopings.

has been reproduced by the simple summation of the spectrum of pure δ -Pu and Am⁹.

Our LDA+DMFT results in Fig. 2 show a very favorable agreement with experiment. The spectral function of Pu atom, displayed in Fig. 2 (f), is almost unchanged in PuAm alloys. The coherence scale, that determine the temperature below which the Pu moment is screened, remains roughly at 800 K in the alloys. The Am spectra is even more doping independent and shows no appreciate change when alloyed with Pu. This is not surprising since a very large pressure is needed to delocalize Am 5*f* electrons^{24,25}, and only the Am IV phase is known to be itinerant (see Fig.1 for location of Am IV in volume diagram). corresponding to volume of Am IV in Fig. 1. Taking into account that the spectra of both Pu and Am are almost unchanged in alloys, the total DOS can be well approximated by a linear combination of the DOS of the two end compounds, as conjectured in Ref. 9.

In order to gain further insight into the puzzle of

the doping independent coherence scale in $\text{Pu}_{1-x}\text{Am}_x$ compound, we will examine the important factors that govern the screening of the magnetic moments in our LDA+DMFT calculation. The temperature dependence of the spectra and hence the coherence scale is entirely determined by the DMFT self-energy correction Σ , which is a functional of the hybridization function Δ , impurity levels E_{imp} and the screened Coulomb interaction U , i.e., $\Sigma[\Delta, E_{imp}, U]$. U is here kept constant. The hybridization function Δ and impurity levels E_{imp} , determined by Eq. 1, are both quite sensitive to the volume change as well as chemical substitutions, as we will show below.

The coherence scale can be expressed analytically when the following two assumptions are made: a) The atom has $\text{SU}(N)$ symmetry and hence the spin-orbit, crystal field splittings and Hund's coupling are absent, b) the hybridization function Δ is frequency and temperature independent. In this case, the Kondo coherence scale can be estimated by $T_K \sim e^{-1/J}$, where J is

$$J \sim \frac{N}{\pi} \left(\frac{|\Delta''|}{E_{n+1} - E_n} + \frac{|\Delta''|}{E_n - E_{n-1}} \right). \quad (2)$$

and E_n are the atomic energies corresponding to occupancy n , N is degeneracy of the $\text{SU}(N)$ model. In the extreme Kondo limit, the difference in the atomic energies are $E_{n+1} - E_n = U/2$ and $E_n - E_{n-1} = U/2$. The above assumptions are not realistic in Pu because of the strong multiplet effects and the strong frequency and temperature dependence of the hybridization function $\Delta(\omega, T)$. Nevertheless, the formula Eq. 2 gives the hint that the coherence scale is sensitive to the ratio $\langle |\Delta''| \rangle / \Delta E_f$, where $\langle |\Delta''| \rangle$ is average of the hybridization function in some low energy region, and ΔE_f is the difference between the ground state of the atomic f^6 configuration and the ground state of the atomic f^5 configuration. Namely, Pu $5f$ electrons are in mixed-valence state with an average occupancy close to $n_f \approx 5.2^6$ therefore the dominant fluctuations are

$$e + 5f^5 \leftrightarrow 5f^6, \quad (3)$$

where e is a conduction *spd* electron.

In turn, the $5f$ occupancy strongly cooperates with the coherence scale, and the scale is smallest in the Kondo regime where n_f is integer. In Fig. 3 (a) we show the $5f$ occupancy for three different cases of chemical substitution and volume change. If the volume of the elemental Pu is changed without alloying, n_f is slightly decreasing with increasing volume (see red curve in Fig. 3 (a)). This is to be expected since in the extreme limit of large volume the system will be in the extreme Kondo limit with $n_f = 5$. The magnitude of the n_f variation in the range of volumes, corresponding to α -Pu and Am is however surprisingly small, only of the order of 0.06. If the volume is kept constant, but the the chemical composition is varied, the occupancy n_f is increasing with Am doping (green dots in Fig. 3 (a) correspond to $x = 0, 1/4, 1/2,$ and $3/4$ from left to right). The Pu atom is thus more

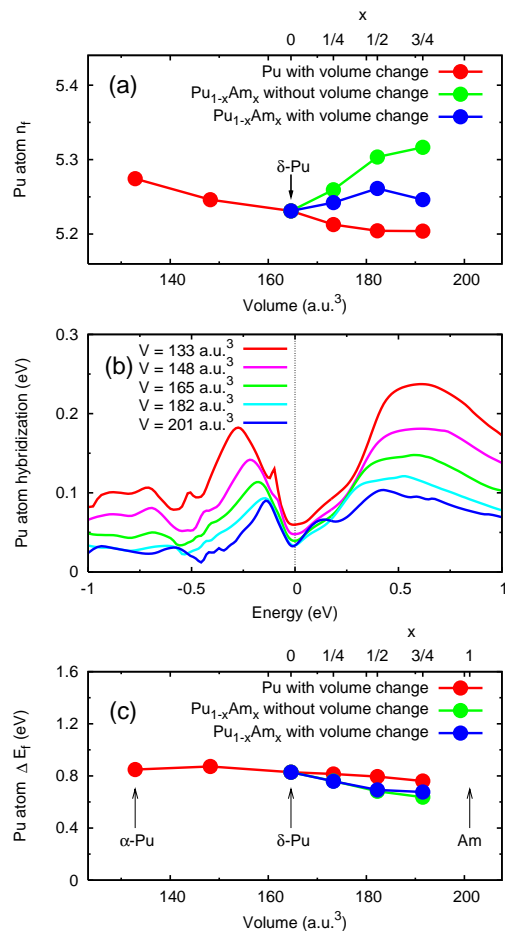


FIG. 3: (a) The number of $5f$ electrons, n_f , as a function of volume (red dots), doping x at constant volume (green dots), and combination of both (blue dots). Note that $a = 8.1, 8.7$ and 9.3 a.u. correspond to the volume of α -Pu, δ -Pu and β -Am, respectively. (b) Volume dependence of hybridization function for Pu in *fcc* phase. (c) The energy difference between the two most relevant atomic states, defined in the text.

mixed valent in the limit of small Pu concentration, i.e., single impurity limit. This might seem counter-intuitive, but the increase in the coherence scale can be understood from the following consideration. The quasiparticle peak detected in $5f$ partial DOS creates a depletion in the conduction *spd* bands. This is traditionally called Kondo hole, which is always pinned at the Fermi level. The hybridization is thus decreased due appearance of quasiparticle peak, an effect termed by Noziere as “exhaustion”. This Kondo hole does not form on Am atom, since there is no coherence peak on Am atom. Thus, if a single Pu atom in emerged in a lattice of Am atoms, the moment can be more efficiently screened by *spd*-electrons, residing on neighboring Am sites. Finally the blue dots in Fig. 3 (a) show that the two effects largely cancel, when both the substitution and volume change are taken into account, and the $5f$ occupancy of $\text{Pu}_{1-x}\text{Am}_x$ is almost constant.

The frequency dependent hybridization function $|\Delta''(\omega)|/\pi$ for elemental Pu at different volumes (no alloying), is shown in Fig. 3 (b). The Kondo hole, i.e., depletion of hybridization at zero frequency, is clearly visible. Moreover, the hybridization changes substantially when volume is varied between the volume of α -Pu and Am volume. The change is between 30% at low energy and up to 50% at intermediate energies. This is a substantial change, which indeed unscreens magnetic moments and changes Pauli susceptibility into Curie-Weiss susceptibility, as shown in Ref. 7.

The Eq. 2 reveals that the coherence scale depends sensitively on the ratio $|\Delta''|/\Delta E_f$ rather than on the hybridization itself. In Fig. 3 (c) we plot the smallest energy difference $\Delta E_f = E_6 - E_5$, which is the dominant contribution to the exchange coupling in Eq. 2. Here E_6 and E_5 are the ground state energies of the atomic f^6 and atomic f^5 configuration, respectively. In Fig. 3 (c) we separate the effect of volume increase from the chemical substitution. It is clear from Fig. 3 (c) that the energy difference is almost three times smaller than $U/2 \sim 2.25eV$, the value that corresponds to the extreme Kondo limit. The $5f^6$ atomic configuration has thus substantial overlap with the ground state wave function of the solid, as shown by valence histogram in Ref. 6. It is also apparent from Fig. 3 (c) that the volume increase has only a small effect on this energy difference (red curve). When alloying with Am, the change of ΔE_f is larger (blue dots) and is of the order of 25%. Since ΔE_f is decreasing, it thus partially compensates the decrease of hybridization with pressure, shown in Fig. 3 (b). However, the magnitude of ΔE_f variation is too small to compensate the dramatic change of hybridization.

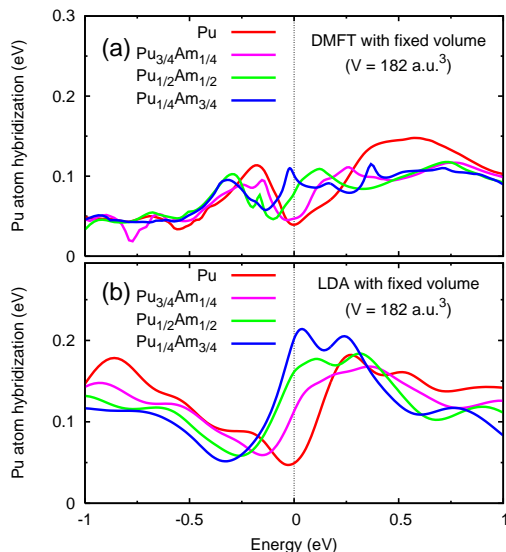


FIG. 4: DMFT hybridization function for $\text{Pu}_{1-x}\text{Am}_x$ at fixed volume (a) computed within the self-consistent LDA+DMFT method, (b) within LDA by setting $\Sigma = 0$.

Finally, Fig. 4a shows the hybridization function for each composition of $\text{Pu}_{1-x}\text{Am}_x$ alloy for the case of a fixed volume. Because the dominant contribution to hybridization function is not the f - f hybridization but the f - spd hybridization¹⁹, the overall magnitude of the hybridization is not changed. However, it is apparent from Fig. 4 (a) that the chemical substitution of Pu by Am eliminates the hybridization dip, and therefore the Pu moment is even more efficiently screened by the spd electrons from neighboring Am atoms than neighboring Pu atoms. This elimination of Kondo hole by the chemical substitution by Am thus compensates the decrease of hybridization due to volume change. The net change of ΔE_f and the change of hybridization $\langle |\Delta''| \rangle$ due to both volume decrease and alloying compensate and lead to a constant coherence scale across the phase diagram.

Fig. 4 (b) shows that the increase of hybridization due to alloying is present even on the LDA level, i.e., computing Δ by Eq. 1 and neglecting the self-energy corrections. However, the magnitude of the hybridization Δ and the magnitude of the change of Δ is substantially larger in LDA than in self-consistent LDA+DMFT method. The “need for renormalization” of the LDA hybridization was pointed out very early on^{26,27} in the context of the description of cerium photoemission, when compared to a single impurity calculations.

To conclude, LDA+DMFT accounts for all the salient features of the experiments, and give new insights into the mechanism for spin compensation in the late actinides. It isolates two essential elements for the screening of the magnetic moment: hybridization and position of the f level. While hybridization is decreased by volume expansion, as naively expected, the substitution of Am eliminates the dip in the hybridization function, and at the same time shifts the position of f level. The three effects compensate each other, and the coherence scale remains around 800 K. Hence the Pu-Am mixtures accentuates the mixed valent character of Pu.

Our work has important experimental consequences. While thermodynamic quantities such as susceptibility and specific heat should not exhibit significant modifications upon alloying, the same is not true for transport quantities. Optical conductivity is an excellent probe of the hybridization gap, and we predict that upon alloying, this hybridization gap will diminish while the dc resistivity will rapidly increases.

Acknowledgment: We acknowledge useful discussions with J. Allen and C. Marianetti. This work was funded by the NNSA SSAA program through DOE Research Grant DE-FG52-06NA26210.

-
- ¹ B. Johansson, *Philos. Mag.* **30**, 469 (1974).
- ² I. V. Solovyev, A. I. Liechtenstein, V. A. Gubanov, V. P. Antropov, and O. K. Andersen, *Phys. Rev. B* **43**, 14414 (1991); A. L. Kutepov and S. G. Kutepova, *J. Phys.: Condens. Matter* **15**, 2607 (2003); P. Soderlind, O. Eriksson, B. Johansson, and J. M. Wills, *Phys. Rev. B* **55**, 1997 (1997); P. Soderlind, *Europhys. Lett.* **55**, 525 (2001).
- ³ J. C. Lashley *et al.*, *Phys. Rev. Lett.* **91**, 205901 (2003).
- ⁴ R. H. Heffner *et al.*, *Phys. Rev. B* **73**, 094453 (2006).
- ⁵ K. T. Moore *et al.*, *Phys. Rev. Lett.* **90**, 196404 (2003); G. van der Laan *et al.*, *Phys. Rev. Lett.* **93**, 097401 (2004); J. G. Tobin *et al.*, *Phys. Rev. B* **72**, 085109 (2005); K. T. Moore *et al.*, *Phys. Rev. B* **73**, 033109 (2006);
- ⁶ J. H. Shim, K. Haule, and G. Kotliar, *Nature* **446**, 513 (2007).
- ⁷ C.A. Marianetti, K. Haule, G. Kotliar, and M.J. Fluss, arXiv:0805.1604 (2008).
- ⁸ G. Chapline, M. Fluss, S. McCall, *J. Alloys and Comp.* **444-445**, 142 (2007).
- ⁹ N. Baclet *et al.*, *Phys. Rev. B* **75**, 035101 (2007).
- ¹⁰ F. H. Ellinger, K. A. Johnson, and V. O. Struebing, *J. Nucl. Mat.* **20**, 83 (1966).
- ¹¹ P. Javorsky, L. Havela, F. Wastin, E. Colineau, and D. Bouexiere, *Phys. Rev. Lett.* **96**, 156404 (2006).
- ¹² A. B. Shick, V. Drchal, and L. Havela, *Europhys. Lett.* **69**, 588 (2005).
- ¹³ L. V. Pourovskii *et al.*, *Europhys. Lett.* **55**, 705 (2006).
- ¹⁴ L. V. Pourovskii *et al.*, *Phys. Rev. B* **75**, 235107 (2007).
- ¹⁵ J.X. Zhu *et al.*, *Phys. Rev. B* **76**, 245118 (2007).
- ¹⁶ A. Georges, G. Kotliar, W. Krauth, and M. J. Rozenberg, *Rev. Mod. Phys.* **68**, 13 (1996).
- ¹⁷ G. Kotliar *et al.*, *Rev. Mod. Phys.* **78**, 865 (2006).
- ¹⁸ S. Y. Savrasov, *Phys. Rev. B* **54**, 16470 (1996).
- ¹⁹ A. Toropova, C.A. Marianetti, K. Haule, G. Kotliar, *Phys. Rev. B* **76**, 155126 (2007).
- ²⁰ K. Haule, S. Kirchner, J. Kroha, and P. Wölfle, *Phys. Rev. B* **64**, 155111 (2001).
- ²¹ K. Haule, *Phys. Rev. B* **75**, 155113 (2007).
- ²² R. D. Cowan, *The Theory of Atomic Structure and Spectra* (Univ. California Press, Berkeley, 1981).
- ²³ S. Y. Savrasov, G. Kotliar, and E. Abrahams, *Nature* **410**, 793 (2001).
- ²⁴ S. Y. Savrasov, K. Haule, and G. Kotliar, *Phys. Rev. Lett.* **96**, 036404 (2006).
- ²⁵ S. Heathman *et al.*, *Phys. Rev. Lett.* **85**, 2961 (2000).
- ²⁶ J. W. Allen, *J. Phys. Soc. Jpn.* **74**, 34 (2005).
- ²⁷ O. Gunnarsson, and K. and Schönhammer, *Phys. Rev. B* **40**, 4160 (1989).